On Conformation and Hydrogen Bonding in Vigabatrin Amino Acid Molecule

N. Sadlej-Sosnowska,* J. Cz. Dobrowolski, W. P. Ozimiński, and A. P. Mazurek

Drug Institute, 30/34 Chełmska Street, 00-725 Warsaw, Poland

Received: December 10, 2001; In Final Form: June 20, 2002

Structure and stability of 285 conformers of the vigabatrin molecule in the gas phase have been obtained by using two combined approaches of conformer search. The first approach consisted of the successive recurrent scanning of all the dihedral angles in the molecule, at the semiempirical AM1 and the ab initio HF/6-31G* levels. The second approach involved the identification of conformers of vigabatrin through the use of a Monte Carlo search coupled with molecular mechanics. The structures formed by using the two kinds of searches were grouped into classes corresponding to defined carbon backbone arrangement and further optimized at the HF/6-311++G** level. For each conformer, if a hydrogen donor−acceptor distance was smaller than ca. 3 Å, the hydrogen bond analysis using the atoms in molecules (AIM) method was applied by using the MP2/6-311++G** electron density. A new intramolecular NH···C hydrogen bonding was found. The selected conformers, being those of the lowest energy in each class and representatives for all kinds of hydrogen bonds, were further optimized at the MP2 level. Parameters of the hydrogen bonds were tabulated, compared, and discussed.

1. Introduction

Vigabatrin (VGB) is a derivative of γ-aminobutyric acid (GABA), the major inhibitory neurotransmitter in mammalian brain. Because there had appeared a suggestion that epilepsy and degenerative disorders of motor control are associated with GABAergic hypofunction, VGB was specially designed to increase levels of GABA within the central nervous system.[1] VGB belongs to the group of a few drugs that were synthesized with a specific targeted mechanism in mind and was subsequently demonstrated to function by that mechanism.[2] VGB replaces GABA as substrate at GABA transaminase, GABA-T, which catabolizes the neurotransmitter degradation to form succinic semialdehyde. However, it possesses an inert appendage at the γ-position, which prevents transamination. Instead, the activated drug bonds covalently to the active site of the enzyme, consuming this enzyme in an irreversible reaction. VGB is generally well tolerated, with a convenient administration schedule, a lack of known significant drug interactions, and no need for routine monitoring of plasma concentration.[3] After 20 years use on humans, it may be concluded that VGB is unlikely to be associated with major adverse effects and may offer tangible improvement in the management of certain types of epilepsy, particularly in case of patients with partial seizures.[3]

Vigabatrin molecule has one chiral center with only an S(+) enantiomer of VGB having the steric properties necessary to be active; however, the drug is administered clinically in a racemic form.

The molecular structure of and atom numbering in the S(+) VGB molecule are shown in Scheme 1. The molecule is characterized by a high degree of flexibility and, due to the presence of carboxylic and amino groups, can give rise to relatively strong intramolecular hydrogen bonds. Both groups can rotate around a covalent C−C and C−N bonds. To our knowledge, no investigations of vigabatrin conformational distributions have been undertaken so far, and the crystallographic structure of solid-state VGB is unknown.

SCHEME 1

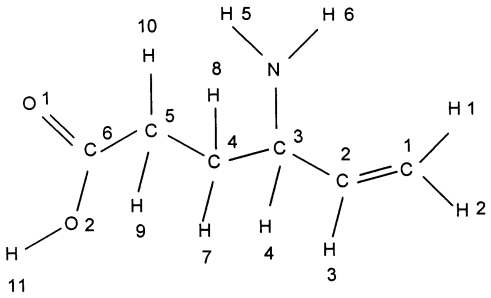

The internal rotation in molecules around the single bonds presents a fundamental problem concerning the nature of noncovalent interactions. This hindering is a purely quantum phenomenon and has no classical analogy.[4] For example, a large rotational barrier of ca. 3 kcal/mol in ethane was measured more than 60 years ago[5] and was rationalized by a hyperconjugation mechanism.[6,7] A great deal of theoretical investigations on molecules is devoted to finding their stable conformers corresponding to local minima on the surface of potential energy of the molecule in the space determined by the rotational degrees of freedom.

Due to the fact that the rotation about C−C as well as C−O and C−N bonds occurring in VGB is not free, only certain values of torsional angles are allowed, and what follows, a large number of stable conformers, corresponding to potential energy minima, can exist.

The aim of the present work was to find as many conformers of the molecule as possible and to understand the factors substantial for their geometric parameters and energy distributions. Our preliminary guess was that the main structural determinant would be the hydrogen bonding.

There are many papers devoted to the collection of the crystallographic data concerning similar H-bond type in different

Corresponding author. E-mail: sadlej@il.waw.pl.

10.1021/jp0144496 CCC: $22.00
Published on Web 10/10/2002

compounds in the solid state. Nevertheless, there has been no such survey for molecules in the gas phase despite the fact that a great number of papers devoted to the conformation and H-bonding in the gas phase were published. We have made such a comparison for different H-bonds in a collection of conformers of a single VGB molecule.

There is no general agreement as to which effects constitute the necessary criteria to conclude that a hydrogen bond is present.

One can conclude about hydrogen bonding via purely geometric criteria as has been frequently done by crystallographers,[8−10] yet the criteria have been recently used for isolated molecules.[11] In the analysis of the crystallographic data the cutoff frequently used is that the hydrogen bonds should be no longer than the sum of van der Waals radii of the atoms involved. The hydrogen bond can also be recognized on the basis of charge density. The first approach to that task is provided by the theory of "atoms in molecules" (AIM).[12−15] The theory was first used to characterize intermolecular hydrogen bonding, but it has also been applied successfully in intramolecular hydrogen bonds.[15] In the framework of the theory, eight concerted effects occurring in the charge density which are indicative of hydrogen bonding were formulated, especially for van der Waals complexes.[14] They were concerned mainly with the topology of the hydrogen bond interatomic surface and properties of the hydrogen atom involved in the bond. AIM analysis is known to be very useful in studying not only strong hydrogen bonding but weaker interactions such as, for instance, C−H···O hydrogen bonds[14−16] or other weak bonds as well.[17] For intramolecular C−H_b···O hydrogen bonds it was found that the charge density of the C−H_b covalent bonds (where H_b refers to the bridging hydrogen) is greater than that of other C−H covalent bonds in the molecule.[15]

The shifts of the electron density in the C−H_b bonds in the intermolecular complexes that result from the formation of the complexing H-bond have also been analyzed by using maps of total electron density. They were displayed by comparing the density in the complex to the same quantity in isolated monomers.[18] In accordance to AIM analysis, this approach has shown that the bridging hydrogen always loses density and that there is a charge buildup along the C−H_b bonds. This charge buildup was also found along the O−H bond in water dimer and it was concluded that the region of charge gain is characteristic of all H-bonds, whether of OH···O or CH···O type.

In the present work, several consecutive criteria were used to pick up the VGB conformers indicating hydrogen bonds. The first criterion was mere geometry: for all conformers where a hydrogen donor−acceptor distance was smaller than ca. 3 Å, the AIM analysis was performed. Fulfilment of this condition also entails that one of the criteria of hydrogen bonding occurrence, within the AIM theory, has to be satisfied: namely, mutual penetration of the hydrogen and acceptor atoms van der Waals envelopes. For example, the sum of the nonbonded radii of O and H atoms, calculated within the theory,[15,19] amounts to ca. 3.1 Å. Next the second discriminant has been used: namely, a critical point on the bond path linking H and an acceptor atom characterized by a positive Laplacian, evaluated at the point. This criterion was considered by Koch and Popelier[14] as a crucial one. At last, other properties calculated within the framework of AIM analysis were considered: charge of the binding hydrogen (ρ_H), charge density of X−H_b bond (ρ_{X-H}), and its Laplacian ($\nabla^2\rho_{X-H}$). They were compared with the same values characterizing nonparticipating H atoms.

2. Methods

In the first approach, the structure was optimized by using the semiempirical AM1 method implemented in Spartan 5.1.[20] The VGB molecule can exist in many different conformations due to the existence of five successive flexible single bonds. There are too many to be scanned simultanously (rotation at 15° scanning step would produce $24^5 \approx 8\,000\,000$ structures). Therefore, to choose the most stable conformer we rotated first two C−C single bonds at 15° steps and optimized $24 \times 24 = 576$ conformers. Then, the lowest energy conformer was selected and the procedure was repeated with the other two C−C single bonds resulting in 576 new conformers. The lowest energy conformer thus obtained at the semiempirical level was used as a starting point for the ab initio calculations. In this conformer the OH, NH_2, COOH, and vinyl groups were further rotated at 15° scanning steps. Rotation of the OH unit in the COOH group (scanning of dihedral angle D1, H11−O2−C6−O1) produced two structures, with parallel and antiparallel arrangement of the C═O and O−H bonds (structures syn and anti). The syn and anti structures were taken separately for further scanning. Rotations of the NH_2, COOH, and vinyl groups were executed by scanning three dihedral angles, D2 (H5−N−C3−C2), D3 (O1−C6−C5−C4), and D4 (N−C3−C2−C1), whereas rotation about C−C bonds was obtained by scanning D5 (C3−C4−C5−C6) and D6 (C2−C3−C4−C5). All the scans were performed at the HF/6-31G* level. The procedure resulted in 107 syn and 119 anti conformers corresponding to the energy minima.

A molecule with as many degrees of freedom as VGB is at the limit of such systematic searching techniques. On the other hand, the stochastic Monte Carlo searching method generally provides a variety of "good structures" with minimal sampling. For that reason, further exploration of the conformational space of the VGB molecule was carried out by the Monte Carlo method implemented in Spartan 5.1, starting with molecular mechanics; the geometries and energies of 61 selected structures (in addition to those found during systematic scanning) were then refined by the ab initio method. To exclude structures that are not stationary points, for all 287 conformers found, the harmonic vibrational wavenumbers were calculated at the HF/6-31G* level. Finally, 285 different structures exhibiting all real harmonic frequencies were further optimized by using the 6-311++G** basis set. The structures fell into a few classes with various backbone arrangements. For their identification, a three-letter acronym specyfying the C3−C4−C5−C6 (lower case), N−C3−C4−C5 (upper case), and C2−C3−C4−C5 (lower case) dihedral angles as trans (t,T), (+)gauche (g, G), or (−)gauche (g′,G′) was used (according to the classification used by Gil et al.[21] for description of structures found for 2-methoxyethanol). The lowest energy conformers in each class were then further optimized at the MP2/6-311++G** level.

The AIM analysis has been performed for all conformers in which a donor−acceptor distance of any anticipated hydrogen bond was lower than ca. 3 Å and for the reference structures belonging to the same class but not exhibiting the relevant H-bond. The hydrogen bond analysis was made with all pertinent conformers to make sure that even small changes of the relevant parameters for weak bonds are meaningful. The AIM analysis was performed by using the electron densities from the MP2/6-311++G** single point calculations. Finally, for each type of hydrogen bond which has been found in the VGB molecule, the AIM analysis was performed after MP2/6-311++G** geometry reoptimization for one exemplary conformer.

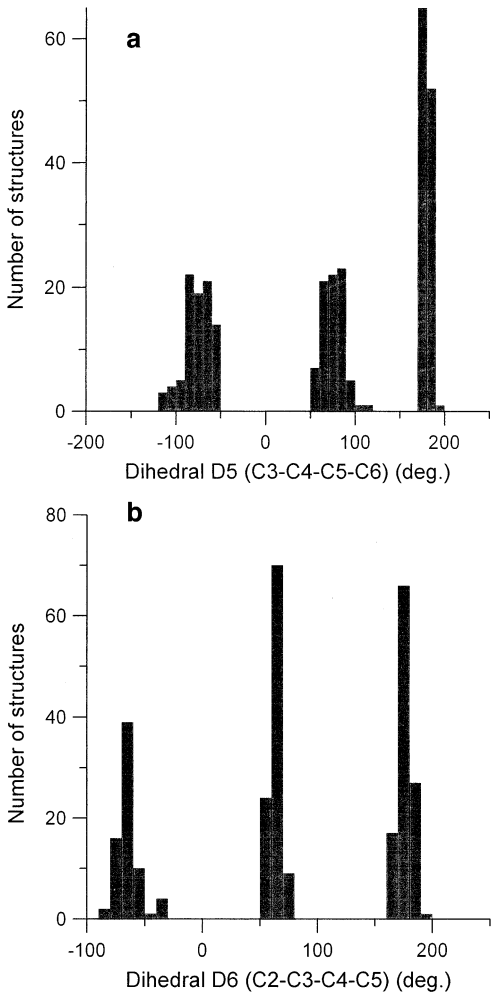

Figure 1. Distribution of dihedral angles of the backbone skeleton: C3−C4−C5−C6 (a) and C2−C3−C4−C5 (b).

The ab initio and AIM calculations[22] were performed by using the Gaussian 98 package[23] running on a SGI computer.

3. Results

3.1. Investigation of VGB Conformational Space. In the whole set of VGB conformers, nine different backbone arrangements were found, namely, gG′t, gTg, tG′t, tGg′, g′Tg, g′G′t, g′Gg′, gGg′, and tTg. The distributions of C3−C4−C5−C6 and C2−C3−C4−C5 dihedral angles of the backbone skeleton are shown in Figure 1. Figure 1a reveals a significant population of trans orientations (117 structures, vs 88 (−)gauche and 80 (+)gauche). On the basis of the behavior of normal alkanes, in which the anti configuration is ca. 0.9 kcal/mol more stable than the gauche configuration,[24] one would predict that the lowest energy conformation of VGB should exhibit two C−C−C−C dihedral angles of 180°. In fact, the most stable conformer of the tG′t class is less stable than the most stable conformer of the gG′t class (1.40 kcal/mol at the MP2/6-311++G** level). The dihedral angle distribution patterns in Figure 1 are different from that found for *N*,*N*,*N*′,*N*′-tetramethylsuccinamide[25] in that they indicate three preferred orientations separated by the void spaces, whereas in the latter the corresponding angles were more evenly distributed (as vigabatrin conformer number is 13 times larger than that of *N*,*N*,*N*′,*N*′-tetramethylsuccinamide, the opposite tendency should be expected).

Conformers within each class differed in values of the D1, D2, D3, and D4 dihedrals. To find all the possible conformers, all dihedral angles were scanned. The potential energy plot for the scan of the −OH unit in the −COOH group is shown in Figure 2, which reveals that the syn structures are energetically favored by ca. 6 kcal/mol. D2, D3, and D4 angles were scanned recurrently and showed one, two, three, and (in one case) four minima. This way the maximum number of conformers within each group could be equal to 3 × 3 × 3 (for syn) and 3 × 3 × 4 (for anti). Actually, the maximum number of conformers in a class equaled 18.

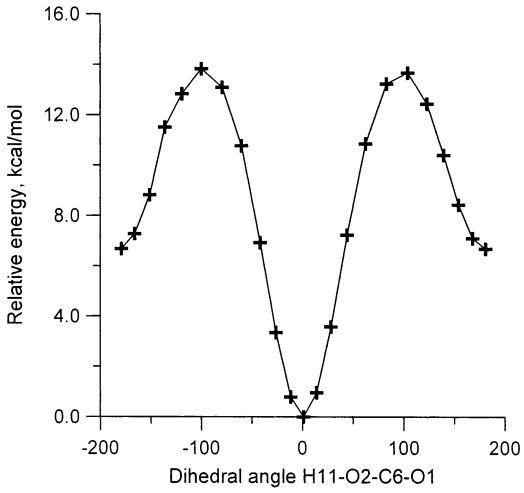

Figure 2. Rotational potential energy plot for the C6−OH bond.

After all the scans, the most stable conformer was the same as that found at the semiempirical AM1 level. The total number of conformers found was 229.

As the number of conformers of the VGB molecule is at the limit of the systematic conformational searching method, the second approach, the Monte Carlo stochastic search, was used for the determination of the preferred geometries. The searching was carried out several times by using different conformers as starting points. Every time the number of conformers found was different, ranging between 113 and 203. The Monte Carlo sets were compared with the results of the previous systematic scanning and 61 new structures were found, namely, 22 anti and 39 syn. Thus the total number of the conformers found equaled 287. After removing two conformers with imaginary frequencies, the remaining 285 structures were reoptimized at the HF/6-311++G** level and their energies recompared; the structure of the lowest energy conformer remained the same at the highest level of theory used.

3.2. Dihedral Angle and Energy Distribution. The energy distributions for the ensamble of syn and anti structures of the VGB conformers are shown in Figure 3. For the syn structures, the conformer energies cover the range 0−6.2 kcal/mol and have a maximum at ca. 2.8 kcal/mol, whereas for the anti conformers, the energies range between 3.5 and 12.1 kcal/mol with a maximum at ca. 9.8 kcal/mol.

Figures 4−6 show the distribution of dihedrals D2′, D3, and D4, corresponding to the NH_2, COOH, and $CH{=}CH_2$ group rotation, respectively (dihedral D2′ differs from D2 (H5−N−C3−C2), in that its first axis is not H−N (because there are two hydrogen atoms bonded to N), but it is rather the n−N axis pointing toward the N atom lone pair. Distribution of the D3 (O1−C6−C5−C4) dihedral is less spiky than the other distributions, yet it also diplays three distinct maxima.

3.3. Hydrogen Bonds. *3.3.1. AIM Analysis*. The presence or absence of the hydrogen bonds often influences markedly the energetic preferences among different conformers of chemical species.

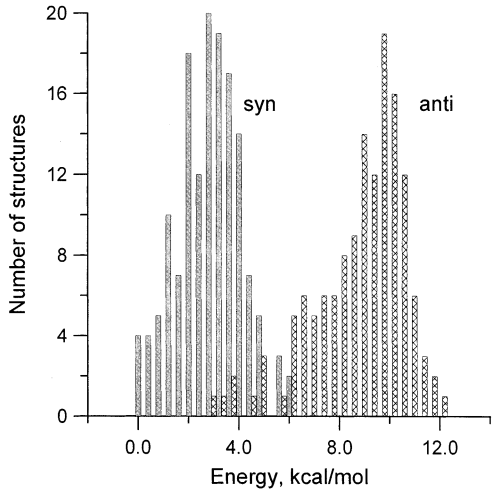

Figure 3. Energy distributions for the syn and anti vigabatrin conformers.

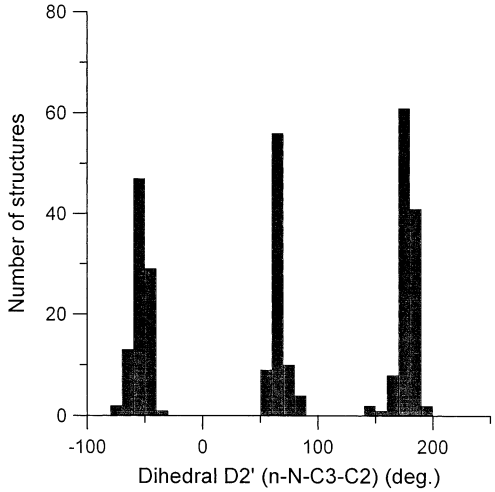

Figure 4. Distribution of D2′ (n−N−C3−C2) dihedrals.

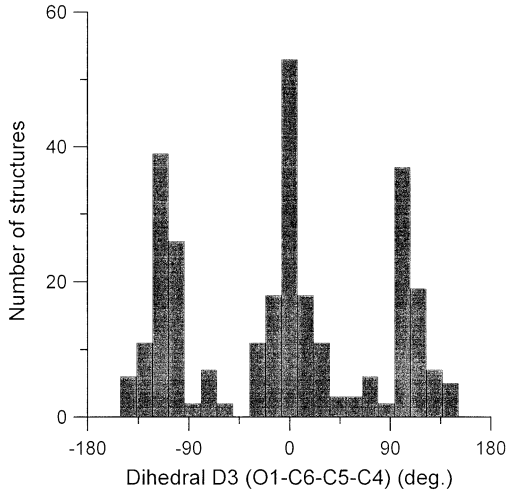

Figure 5. Distribution of D3 (O1−C6−C5−C4) dihedrals.

Vigabatrin, possessing nine heavy atoms, is a rather small molecule. Still seven types of intramolecular hydrogen bonds have been found among the set of its conformers. Now, the hydrogen bonds found in VGB according to criteria elaborated by AIM theory (critical point on the path connecting H and an acceptor, H···A; positive Laplacian of the electron density ρ_b at that point, $\nabla^2\rho_b$; loss of electron density on H; systematic

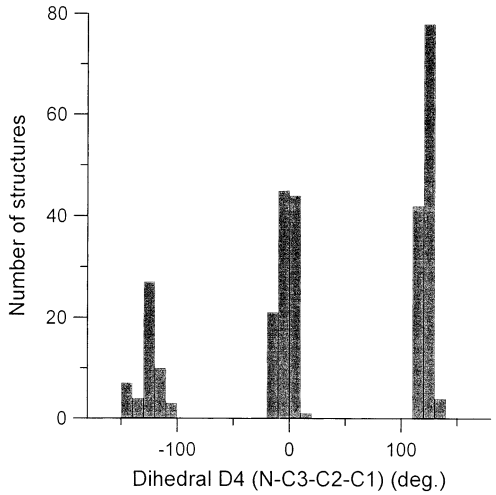

Figure 6. Distribution of D4 (N−C3−C2−C1) dihedrals.

TABLE 1: AIM Analysis of the Hydrogen Bonds Critical Points Found in VGB Conformers[a]

		H-bond critical point	
bond	*n*	ρ_b	$\nabla^2\rho_b$
OH···N	11	0.0309	0.0865
	1	*0.0480*	*0.1072*
OH···π	6	0.0101	0.0281
	1	*0.0167*	*0.0463*
NH···O=C	13	0.0093	0.0334
	1	*0.0172*	*0.0629*
NH···C(O)OH	3	0.0087	0.0304
	1	*0.0108*	*0.0368*
CH4···O=C	3	0.0087	0.0314
	1	*0.0103*	*0.0309*
NH···OH	9	0.0072	0.0253
	1	*0.0113*	*0.0394*
CH3···O=C	4	0.0066	0.0242
	1	*0.0058*	*0.0202*

[a] At the MP2/6-311++G**//HF/6-311++G** level (upper lines) and at the MP2/6-311++G** level (italics). ρ_b (e Bohr^{-3}); $\nabla^2\rho_b$ (e Bohr^{-5}).

changes of the electron density of the X−H covalent bond critical point) will be considered in the order from the strongest to the weakest one. This ordering was indicated by the value of the electron density ρ_b, because it was found that there are correlations between its values and H-bond energies.[26,27] In some cases the AIM code failed, when the atomic surface sheet could not be determined due to iterative divergence; nevertheless, in the course of this procedure, we were able to select the systems possessing H-bonding among a great number of all conformers.

Values of ρ_b and $\nabla^2\rho_b$ are shown in Table 1. It can be seen that except for the OH···N bond, all the other H-bonds are of similar strength. The values of the Laplacian are positive: this indicates that the interaction is dominated by the contraction of charge density away from the interatomic surface, which leads to the accumulation of charge in separate atom basins. The steeper the walls of a well thus formed, the more positive the $\nabla^2\rho_b$. Typically, the densities ρ_b are approximately an order of magnitude smaller than those found for the covalent bonds, which means that they are relatively low.

The AIM analysis additionally showed that the existence of H-bonding can also be deduced from the properties of the critical points on the attractor interaction lines corresponding to Lewis covalent bonds. This procedure was applied by Popelier and

TABLE 2: Analysis of the Critical Points of the O−H and C−N Covalent Bonds Engaged in OH···NC Hydrogen Bond and of Reference O−H and C−N[a]

range of OH···NC distances	*n*	OH covalent bond critical point			CN covalent bond critical point	
		ρ_H	ρ_{O-H}	$\nabla^2\rho_{O-H}$	ρ_{C-N}	$\nabla^2\rho_{C-N}$
1.91−1.94	11	0.4076	0.3631	−2.653	0.2582	−0.6898
1.75	1	*0.3742*	*0.3264*	*−2.261*	*0.2492*	*−0.6323*
>3.3	7	0.4332	0.3813	−2.756	0.2688	−0.7429
3.67	1	*0.4157*	*0.3603*	*−2.512*	*0.2665*	*−0.7246*
difference		−0.0256	−0.0182	0.103	−0.0106	0.0531
		−0.0415	*−0.0339*	*0.251*	*−0.0173*	*0.0923*

[a] Calculations at the MP2/6-311++G**//HF/6-311++G** level (upper lines) and at the MP2/6-311++G** level (italics). ρ_b (e Bohr^{-3}); $\nabla^2\rho_b$ (e Bohr^{-5}).

TABLE 3: Analysis of the Critical Points of the O−H Covalent Bonds Engaged in OH···π Hydrogen Bonds and in Reference O−H[a]

range of OH···C(sp^2) distances	n	covalent bond critical point		
		ρ_H	ρ_{O-H}	$\nabla^2\rho_{O-H}$
2.49−2.54	6	0.4280	0.3784	−2.748
2.27	1	*0.4069*	*0.3546*	*−2.495*
> 3.53	6	0.4344	0.3823	−2.760
3.45	1	*0.4165*	*0.3608*	*−2.513*
difference		−0.0064	−0.0039	0.012
		−0.0096	*−0.0062*	*0.018*

[a] Calculations at the MP2/6-311++G**//HF/6-311++G** level (upper lines) and at the MP2/6-311++G** level (italics). ρ_b (e Bohr^{-3}); $\nabla^2\rho_b$ (e Bohr^{-5}).

TABLE 4: Analysis of the Critical Points of the N−H Covalent Bonds Engaged in NH···O=C Hydrogen Bonds and in Reference N−H[a]

range of NH···O=C distances	*n*	covalent bond critical point		
		ρ_H	ρ_{NH}	$\nabla^2\rho_{NH}$
2.21−2.78	13	0.4349	0.3462	−1.698
2.19	1	*0.4207*	*0.3332*	*−1.594*
≥3.2	13	0.4376	0.3455	−1.653
3.76	1	*0.4272*	*0.3326*	*−1.507*
difference		−0.0027	0.0007	−0.045
		−0.0065	*0.0006*	*−0.087*

[a] Calculations at the MP2/6-311++G**//HF/6-311++G** level (upper lines) and at the MP2/6-311++G** level (italics). ρ_b (e Bohr^{-3}); $\nabla^2\rho_b$ (e Bohr^{-5}).

Bader in the investigation of CH···O bonding in creatine and sarcosine.[15] Values of Laplacian of the covalent bond critical points are negative, pointing at the maximum electron density.

The properties of the covalent bond critical points are summarized in Tables 2−9. Values given in Tables 2−8 represent the averages calculated only for these conformers which the AIM analysis showed to possess the critical point on the hydrogen bond path (*n* is the number of such conformers). Among the conformers with CH7···O=C distances shorter than 2.8 Å, no critical point at the hydrogen bond path was found. Nevertheless, the parameters of the C−H7 covalent bond and ρ_H followed the same trend as of N−H, C−H3, and C−H4, forming hydrogen bonds (Tables 4−8). That is why the corresponding mean values for the conformers showing short CH7···O=C distance are also tabulated (Table 9).

3.3.2. The OH···N Hydrogen Bond. From the data of Table 1 it can be seen that the OH···N hydrogen bond is the strongest.

TABLE 5: Analysis of the Critical Points of the N−H Covalent Bonds Engaged in NH···C(O)OH Hydrogen Bonds and in Reference N−H[a]

range of NH···C(O)OH distances	*n*	covalent bond critical point		
		ρ_H	ρ_{N-H}	$\nabla^2\rho_{N-H}$
2.68−2.71	3	0.4355	0.3463	−1.691
2.55	1	*0.4251*	0.3331	*−1.537*
≥3.2	3	0.4364	0.3444	−1.646
3.0	1	*0.4257*	*0.3314*	*−1.496*
difference		−0.0009	0.0019	−0.045
		−0.0006	*0.0017*	*−0.041*

[a] Calculations at the MP2/6-311++G**//HF/6-311++G** level (upper lines) and at the MP2/6-311++G** level (italics). ρ_b (e Bohr^{-3}); $\nabla^2\rho_b$ (e Bohr^{-5}).

TABLE 6: Analysis of the Critical Points of the C−H4 Covalent Bonds Engaged in CH4···O=C Hydrogen Bonds and in Reference C−H4[a]

range of CH4···O=C distances	*n*	covalent bond critical point		
		ρ_H	ρ_{C-H4}	$\nabla^2\rho_{C-H4}$
2.63−2.65	3	0.4392	0.2861	−1.000
2.51	1	*0.4326*	*0.2803*	*−0.962*
≥3	6	0.4392	0.2827	−0.977
3.10	1	*0.4334*	*0.2732*	*−0.910*
difference		0.0000	0.0034	−0.023
		−0.0008	*0.0071*	*−0.052*

[a] Calculations at the MP2/6-311++G**//HF/6-311++G** level (upper lines) and at the MP2/6-311++G** level (italics). ρ_b (e Bohr^{-3}); $\nabla^2\rho_b$ (e Bohr^{-5}).

TABLE 7: Analysis of the Critical Points of the N−H Covalent Bonds Engaged in NH···OH Hydrogen Bonds and in Reference N−H[a]

range of NH···OH distances	*n*	covalent bond critical point		
		ρ_H	ρ_{N-H}	$\nabla^2\rho_{N-H}$
2.43−2.80	9	0.4363	0.3461	−1.677
2.35	1	*0.4236*	*0.3327*	*−1.548*
≥4	9	0.4374	0.3456	−1.656
3.95	1	*0.4271*	*0.3323*	*−1.502*
difference		−0.0011	0.0005	−0.021
		−0.0035	*0.0004*	*−0.046*

[a] Calculations at the MP2/6-311++G**//HF/6-311++G** level (upper lines) and at the MP2/6-311++G** level (italics). ρ_b (e Bohr^{-3}); $\nabla^2\rho_b$ (e Bohr^{-5}).

This bond was found in anti structures only, where the OH group is not engaged in the attractive interactions with the C=O group. The bond was found for five conformers of the g′Gg′ class and three in the gG′t and g′G′t classes each. One exemplary conformer with the OH···N hydrogen bond is shown in Figure 7.

In Table 2 the critical point parameters of the O−H and C−N covalent bonds, adjacent to the OH···NC hydrogen bond, are shown and compared with the parameters for a sample of conformers not forming any H-bond of this kind. Table 2 also lists differences in the several parameters characterizing systems with and without the OH···N bonding. It can be seen that upon H-bond formation, the values of ρ_H, ρ_{OH}, and ρ_{CN} decrease, indicating an outflow of electron density from these points toward the remainder of the molecule (see also ρ_b for the OH···N hydrogen bond, Table 1). This loss of charge of the H atom is one of the H-bond formation criteria.[14] Upon H-bond

TABLE 8: Analysis of the Critical Points of the C−H3 Covalent Bond Engaged in CH3···O═C Hydrogen Bonds and in Reference C−H3[a]

range of CH3···C═O distances	*n*	covalent bond critical point		
		ρ_H	ρ_{C-H3}	$\nabla^2\rho_{C-H3}$
2.70−3.03	4	0.4323	0.2830	−0.987
2.78	1	*0.4245*	*0.2773*	*−0.949*
≥3.3	3	0.4329	0.2811	−0.975
3.47	1	*0.4271*	*0.2749*	*−0.932*
difference		−0.0006	0.0019	−0.012
		−0.0026	*0.0024*	*−0.017*

[a] Calculations at the MP2/6-311++G**//HF/6-311++G** level (upper lines) and at the MP2/6-311++G** level (italics). ρ_b in (e Bohr^{-3}), $\nabla^2\rho_b$ in (e Bohr^{-5})

TABLE 9: Analysis of the Critical Points of the C−H7 Covalent Bonds and of Reference C−H8[a]

range of CH···O═C distances	*n*	covalent bond critical point			
		ρ_H	d_{C-H7}	ρ_{C-H7}	$\nabla^2\rho_{C-H7}$
2.48−2.74	8	0.4316	1.084	0.2806	−0.961
≥3.8	8	0.4341	1.086	0.2786	−0.948
difference		−0.0025	−0.002	0.0020	−0.013

[a] Calculations at the MP2/6-311++G**//HF/6-311++G** level. Bond lengths d_{C-H7} in angstroms. ρ_b (e Bohr^{-3}); $\nabla^2\rho_b$ (e Bohr^{-5}).

formation, the OH and NC bonds are elongated (Figure 8). The Laplacian of the electron density at the critical point of both bonds is less negative, indicating that the covalent bond electron density is more diffused in the vicinity of the maximum. The OH bond and CN bonds are weakened.

3.3.3. The OH···π Hydrogen Bond. During the past decade the investigations of H-bond interactions have shown that the concept of (X−H···Y) hydrogen bonding, where X and Y are the electron withdrawing atoms, is not complete and can be extended to the interactions with π charge distributions (Y−π-electron system). Experimentally, such interactions were studied using rotational spectroscopy (HOH···benzene),[28] X-ray analysis (HOH···calix[4]arene,[29] some terminal alkynes,[30] mestranol[31]), and neutron diffraction (stacked molecules of 1,8-bis-(dimethylamino)naphthalene[32]). Cambridge Structural Database analysis resulted in finding O−H···C═C, N−H···C═C, O−H···C/C, and N−H···C/C bonds.[9]

On the basis of the NMR high-field shift of ethinyl protons, the intermolecular H···π bonding in phenylacethylene was found.[33] The same bonding involving π electrons of the benzene ring in 2-phenylpropionaldehyde and 9-(2-alkylphenyl)fluorene[34] was proposed, as were CH/n interactions, involving unshared electrons of O atoms in alcohols and ketones.[34,35]

The π-type hydrogen bonded systems consisting of acetylene, ethylene, cyclopropane, and benzene as proton acceptors and hydrogen halides as proton donors have been studied theoretically by means of the ab initio method since 1982.[36−40] The same bonding in a number of other complexes was also investigated.[9,40−43]

Characteristics of the π-type hydrogen bonding in VGB (between hydrogen of the OH group and one of the sp^2 carbons of the vinyl group) are given in Tables 1 and 3. The distances between H atom from the OH moiety were closer to CH than to CH_2 vinyl carbon atoms (2.49−2.54 and 2.66−2.91 Å, respectively). One of the VGB conformers forming the OH···π bonding is shown in Figure 7. Optimization at the MP2 level resulted in the shortening of the OH···C(sp^2) distances from 2.50 and 2.68 Å to 2.27 and 2.44 Å, respectively.

In the conformers where the OH group hydrogen atom is involved in the H-bonding, the electronic charge at the H atom (of the OH group) decreases by 0.0064 *(0.0096)* au upon H-bond formation. Here, and further on, an applied convention is that the first value regards a mean for all critical points found by using electron densities from MP2/6-311++G** single-point calculations (geometry optimized at HF/6-311++G** level), whereas the second, in *italics*, concerns two selected conformers−with and without a given hydrogen bond, optimized at MP2/6-311++G** level prior to AIM analysis. The value of ρ_{OH} for the O−H_b bond is lower than that for the other ones by 0.004 *(0.006)* au. This implies that the O−H bond is slightly weakened. It is consistent with the lengthening of the OH bond upon hydrogen bond formation (Figure 8). Nevertheless, the bond is weakened far less than in the case of the OH···N bonding. A slight decrease of the absolute value of the charge density Laplacian at the OH bond critical point, by 0.0012 (*0.0018*) au, shows that with the H-bond formation the electronic charge is a little less concentrated (or more diffused to a small degree). This is also consistent with the lengthening of the OH covalent bond. Although these differences between conformers forming or not forming the OH···π H-bond are small, they are systematic and statistically significant. For comparison, the increments of the critical point properties of the C−H bond upon formation of the H_3C−H···π complexes with benzene ring were, $\Delta\rho$, 0.002, and, Δ Laplacian, −0.02.[40]

3.3.4. The NH···O and CH···O Hydrogen Bonds. In the most conformers forming the NH···O═C or NH···OH hydrogen bonds, either the CH···O═C or CH···OH hydrogen bond was also found and vice versa. What follows, the effects resulting from one type of the H-bonding may be influenced by the second type of H-bonding. Data for the H-bonds are collected in Tables 1, 4, and 6−8. In the tables, only those conformers are gathered in which the H-bond critical point (Table 1) was found, but the total number of conformers with the CH4···OH, NH···OH, CH4···O═C, and CH4···OH distances shorter than the sum of the experimental[44] or theoretical[15,19] nonbonded atomic radii was much larger. The CH4 bonds are shortened upon the CH4···O H-bond formation by 0.005 *(0.006)* Å. A slight C−H shortening was also found for the CH3···O═C bond (Figure 8). This implies that the C−H bond is strengthened; this effect was previously found theoretically by Popelier and Bader,[15] Cubero et al.,[40] and Hobza et al.[45] The corresponding values of a C−H bond shortening found by Popelier and Bader were 0.006 and 0.012 Å for creatine and sarcosine, respectively.[15]

On the other hand, while some of the NH bonds are shortened upon H-bond formation, others are lengthened and the mean result is close to zero. After MP2 optimization, the bonds lengthened by only a small amount, *0.001−0.002* Å. ρ_H for the NH···O bond is decreased due to the loss of charge, similarly to the case of the strongest OH···N bonds. The covalent bond parameter changing to a greatest degree upon the H-bonding was the Laplacian of the covalent bond electron density. In all cases its absolute value was significantly larger (up to 5%) for X−H_b bonds than for the reference ones.

The weakest hydrogen bond (Table 1) is the vinyl group CH3···O═C interaction where the C atom has the sp^2 hybridization. Figure 7 represents the conformer with the C(sp^2)H···O═C bonding.

3.3.5. The NH···C(O)OH Hydrogen Bond. To our knowledge, such bonding has not been observed previously, neither experimentally nor theoretically. However, similar NH···C═C, NH···C/C, and NH···phenyl ring bonds have been found in

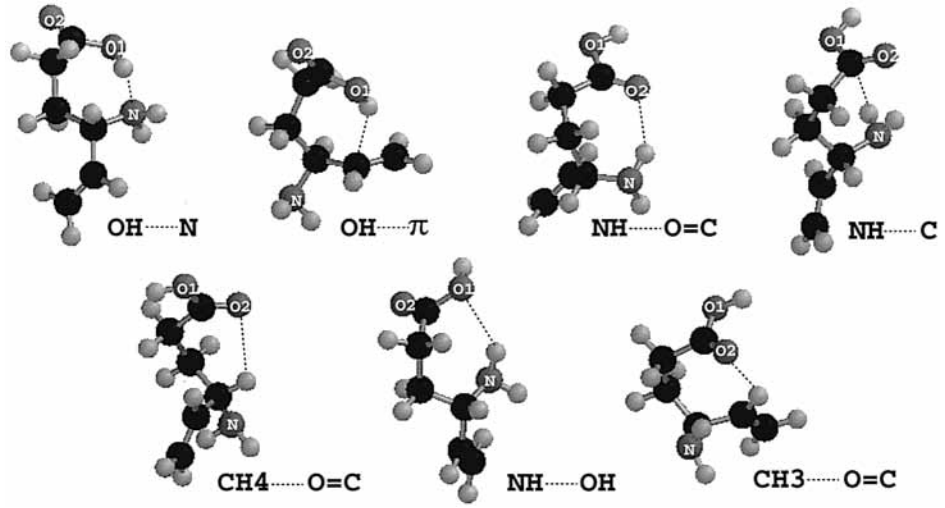

Figure 7. MP2/6-311++G** optimized geometries of vigabatrin conformers representative for the seven types of hydrogen bond found in this work.

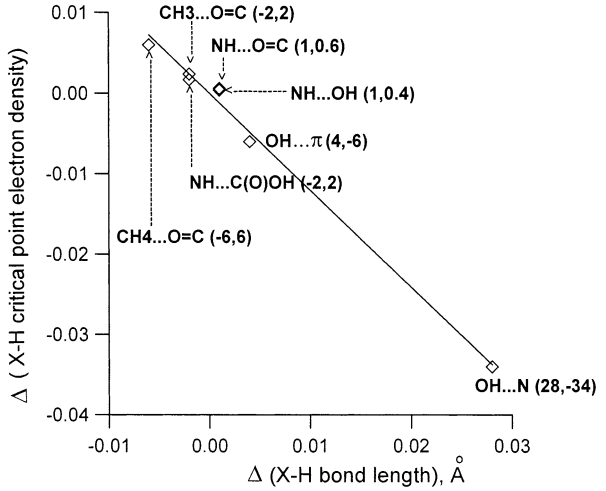

Figure 8. Dependence of the increment of electron density of the covalent bond engaged in a hydrogen bonding on the increment of the bond length, as compared with reference structures. AIM analysis and geometry optimization were at the MP2/6-311++G** level. Values of the variables, multiplied by 1000, are given in parentheses.

crystalline alkynes, alkenes, and aromatics,[9,43] as well as the NH···N bond in 2-aminopropenenitrile[46] and 1*H*-tetrazole.[47] A comparison of the H-bond critical point parameters (Table 1) shows that this bond is of similar strength as the better known NH···O ones. The N−H bond distance and ρ_{N-H} changes upon the NH···C bond formation (Figure 8, Table 5) indicate that the NH bond is strengthened to a minor degree. Frequencies of the N−H bond stretch (at HF/6-311++G** level) are blue shifted (as compared with a reference) by 6.72 and 14.56 cm^{-1}. These value are similar as those for the corresponding shifts for N−H in NH···O═C (5.57 and 17.16 cm^{-1}) and in NH···O−H (14.81 and 6.32 cm^{-1}).

3.3.6. The Putative H Bonds Not Satisfying Some of the Criteria. Critical points on the bond path linking H3 and C6 have been found for two conformers, suggesting existence of the CH3···C(O)OH hydrogen bond. The critical bond parameters were almost the same as those of the NH···C(O)OH bond; electron density of the CH3 bond and its Laplacian changed even more than the corresponding values for NH and in the same direction. The CH3 bond length was shortened by 0.005 (*0.004*) Å. However, after MP2 optimization, the critical point disappeared in one of the conformers; in the other, the electron density on H3 in one of the conformers was higher than that in reference structures. Since this criterion is treated as a very important one,[14,15,18] we can state that this bond is close to nonexistent.

Now let us focus on the $C(4)H_2$ group. In many conformers, one of the CH bonds seems to interact with O═C electron donor center (H atom of that bond is numbered H7; the other, H8). They showed the CH7···O distances in the range for which the critical point was found for another $C(sp^3)H\cdots O$, namely, CH4···O bond (Table 6). The lengths of the presumed H···O hydrogen bond (2.48−2.74 Å) are up to 0.2 Å shorter than the sum of the nonbonded radii for the O and H atoms, provided one takes the experimental atomic radii[44] as a point of reference, or 0.4−0.6 Å in the case where the reference radii are calculated from the wave functions.[19] The difference stems from the fact that the sum of the nonbonded radii of O and H atoms, calculated within the theory,[15,19] is larger than that calculated according to ref 44. However, for the expected CH7···O bonds, no H-bond critical points were found. Further investigation encompassed only those structures where the presumed CH7···O bond was not accompanied, and possibly perturbed, by a CH4···O or NH···O bonding. For such eight conformers the three characteristics mentioned in Table 9: ρ_H, ρ_{CH7}, and $\nabla^2\rho_{CH7}$, were changed in parallel with those for the other CH···O hydrogen bonds (Tables 6 and 8). What is more, the C−H7 bond length (d_{CH7}) was lower than C−H8 when the distance H7···O1 was small. This suggests that also in this case the H-bonding should take place and yet, within the framework of AIM theory, is nonexistent. It seems to us that despite the unequivocal criteria of the H-bond occurrence, sometimes the H-bonding is not merely a yes/no concept; while most conformers undisputably possess an H-bond or not, borderline cases do occur.

3.3.7. Hydrogen Bond X−H···A and the Electron Density of the X−H Bond. There has been a spate of evidence that in a number of C−H···A bonds the interaction with a proton acceptor leads to the shortening of the bridging $C-H_b$ bonds.[15,45,48,49] The blue frequency shift is associated with this bond shortening.[45,48,49] However, there also exist (and were the first to be recognized) other hydrogen bonds, as O−H···O,[10] where the lengthening of $X-H_b$ and the bond frequency red shift has been evidenced. Recent calculations of the electron density for the sets of C−H···O with C−H contracting bonds and for another set with C−H lengthening bonds, as well as for a water dimer,

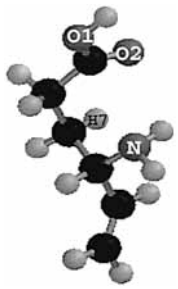

Figure 9. Vigabatrin conformer of the lowest energy in the gas phase.

revealed that the density shifts of blue- and red-shifting H-bonds are very much alike.[18] In particular, the charge buildup was found along the covalent X−H bond. The authors used the maps of total electron density in space and investigated the intermolecular H-bonding. They stated that their finding belies the notion that the stretching that occurs in the equilibrium length of the O−H bond as well as the red shift of the O−H stretching frequency can be attributed to a loss of density in the O−H binding area.

The results of the present AIM analysis of different intramolecular hydrogen bonds in VGB are not in parallel with that finding. Comparison of data in Tables 2 and 3 with those in Tables 4−8 shows that for the first two hydrogen bonds, OH···N and OH···π, the O−H bond critical point electron density is lower than that in the isolated O−H bonds.

What is more, the absolute value of its Laplacian is also lower, pointing at the more diffuse electron distribution in the critical point vicinity. On the other hand, for the rest of the hydrogen bonds, changes of the opposite direction have been found. Figure 8 presents the plot of the electron density increment in the X−H_b covalent bond vs the increment of the X−H length. The electron density change is significant (higher than 1 mÅ) for five bonds; that for NH···O═C and NH···OH is negligible. The two bonds on the right are characterized by the lengthening of the O−H bonds and diminishing ρ_{O-H}, the rest by the shortening of C−H and N−H bonds, accompanied by the increase in ρ_{X-H}. To sum up, the AIM consideration of the electron density lets us believe that density in the region between the O and H_b atoms is not increased, contrary to what has been claimed in ref 18 but in accordance with an estimation of strength of intramolecular hydrogen bonds.[50]

3.3.8. Hydrogen Bonding and Stabilization Energy. In the lowest energy conformer, two distances were found to be short enough, 2.56 and 2.53 Å for the NH···O═C and CH7···O═C moieties, respectively, to presuppose the hydrogen bond interaction (Figure 9). However, no H-bond critical point was found. This suggests that a single effect such as H-bonding cannot determine the stabilities of the different conformations for such a molecule as VGB. From the analysis of the optimized structures, it emerges that an important structural feature for energy stabilization is the orientation of the lone pair of the amino group relative to the π electrons of the vinyl group.

4. Conclusions

This study has identified 285 gas-phase minima for vigabatrin. The results given in Figures 1, 2, and 4−6 evidence rotational barriers found for all the intramolecular rotations and show that these motions are hindered. For every rotation, the maxima and minima of potential energy dependence on the rotational angles occur at similar angles. Thus the histograms of all values of dihedral angles corresponding to rotation around the C−C, C−N, and C−O bonds have three distinct maxima. Due to the fact that the rotation is not free, the maximum number of the possible conformations is quite well-determined.

The Monte Carlo method provided a family of conformers in good agreement with those obtained from the exhaustive search by scanning the individual dihedral angles. Furthermore, most notably, the global minimum found by both approaches was the same. As expected, each method identified many conformers different than those found by the other method. Aiming at finding the largest conformers set as possible, we combined the two methods, but the set obtained by us may yet be incomplete.

In the VGB molecule, hydrogen bonds of seven different kinds were found; among them the intramolecular NH···C(O)OH bonding was found, to our knowledge, for the first time. Only one fairly strong intramolecular H-bonding, the O−H···N bond, was found in the whole conformer family. It diminished energies of the relevant structures by ca. 3−4 kcal/mol. The other hydrogen bonds, OH···π, NH···O, and CH···O, are much weaker, the OH···π being the strongest of the group. We have noted that the formation of the shortest (1.91−1.94, *1.75* Å) and the strongest H-bonds does not occur in conformers with a typical closed six-membered ring arrangement, but it does in those with seven-membered rings (−C−N···H−O−C−C−C−).

The analysis of the electron densities of the covalent X−H_b bond critical points revealed that in O−H···N and O−H···π, the O−H bonds are longer, the critical point electron density and the absolute value of its Laplacian are lower, than the respective values of reference O−H bonds. However, for the CH4···O═C, CH3···O═C, and N−H···C(O)OH bonds, the X−H_b bond parameters change in the opposite direction. This finding would contradict the statement that there is a clear increase of density in the X−H bond of the proton donor molecule, regardless of whether this bond is lengthened, shortened, or left unchanged by its interaction with the proton acceptor molecule.[18] We believe that some important contribution to this discussion could be provided by crystallographers.

The most stable gas-phase conformer exhibits no hydrogen bonding or the bond is so weak that it cannot be detected by using the AIM analysis. The NH_2 group in the VGB molecule is a good hydrogen bond acceptor with much weaker donor properties.

Acknowledgment. N.S.S. kindly acknowledges an inspiring discussion with Prof. Krzysztof Woźniak from the Chemistry Department of the University of Warsaw.

Supporting Information Available: This supplementary material contains: (1) the pdb files of all 285 conformers optimized at the HF/6-311++G** level. The files are grouped in the columns corresponding to the different backbone classes. The files corresponding to different geometries of the COOH group (syn or anti) are gathered in the separate tables. The numbers in the names of the individual pdb files are the relative energies of the conformers, in kcal/mol. (2) The pdb files of the conformers representative for seven types of the hydrogen bond optimized at the MP2/6-311++G** level. This information is available free of charge via the Internet at http://pubs.acs.org.

References and Notes

(1) Grant, S. M.; Heel, R. C. *Drugs* **1991**, *41*, 889.
(2) French, J. A. *Epilepsia* **1999**, *40*, S11.
(3) Gidal, B. E.; Privitera, M. D.; Sheth, R. D.; Gilman, J. T. *Ann. Pharmacother*. **1999**, *33*, 1277.

(4) Dodziuk, H. *Modern Conformational Analysis;* VCH: New York, 1995.
(5) Kemp, J. D.; Pitzer, K. S. *J. Chem. Phys.* **1936**, *4*, 749.
(6) Nakai, H., Kawamura, Y. *Chem. Phys. Lett.* **2000**, *318*, 298.
(7) Pophristic, V.; Goodman, L. *Nature* **2001**, *411*, 565.
(8) Taylor, R., Kennard, O. *J. Am. Chem. Soc.* **1982**, *104*, 5063.
(9) Viswamitra, M. A.; Radhakrishnan, R.; Bandekar, J.; Desiraju, G. R. *J. Am. Chem. Soc.* **1993**, *115*, 4868.
(10) Jeffrey, G. A., Saenger, W., *Hydrogen Bonding in Biological Structures;* Springer-Verlag: New York, 1994.
(11) Vorobyov, I.; Yappert, C.; DuPré, D. B. *J. Phys. Chem. A* **2002**, *106*, 668.
(12) Bader, R. F. W.*Chem. Rev.* **1991**, *91*, 893.
(13) Bader, R. F. W. *Acc. Chem. Res.* **1985**, *18*, 9.
(14) Koch U.; Popelier P. L. A. *J. Phys. Chem.* **1995**, *99*, 9747.
(15) Popelier, P. L. A.; Bader, R. F. W. *Chem. Phys. Lett.* **1992**, *189*, 542.
(16) Sosa G. L.; Peruchena N.; Contreras R. H.; Castro E. A. *J. Mol. Struct.* **1997**, *401*, 77.
(17) Cioslowski, J.; Mixon, S. T.; Edwards, W. D. *J. Am. Chem. Soc.* **1991,** *113*, 1083.
(18) Scheiner S.; Kar T. *J. Phys. Chem. A* **2002**, *106*, 1784.
(19) Bader, R. F. W.; Beddal, P. M.; Cade, P. E. *J. Am. Chem. Soc.* **1991**, *93*, 3095.
(20) Spartan 5.1, Wavefunction, Inc., 18401 Von Karman Ave., Suite 370, Irvine, CA 92612.
(21) Gil, F. P. S. C.; Fausto, R.; Amorim da Costa, A. M.; Teixeira-Dias, J. J. C. *J. Chem. Soc., Faraday Trans.* **1994**, *90*, 689.
(22) (a) Cioslowski, J.; Nanayakkara, A., Challacombe, M. *Chem. Phys. Lett.* **1993**, *203*, 137. (b) Cioslowski, J. *Chem. Phys. Lett.* **1992**, *194*, 73. (c) Cioslowski, J.; Nanayakkara, A. *Chem. Phys. Lett.* **1992**, *219*, 151.
(23) Gaussian 98, Revision A.7, Frisch M. J.; Trucks G. W.; Schlegel H. B.; Scuseria G. E.; Robb M. A.; Cheeseman J. R.; Zakrzewski V. G.; Montgomery J. A.; Stratmann, R. E.; Burant, J. C.; Dapprich, S.; Millam, J. M.; Daniels, A. D.; Kudin, K. N.; Strain, M. C.; Farkas, O.; Tomasi, J.; Barone, V.; Cossi, M.; Cammi, R.; Mennucci, B.; Pomelli, C.; Adamo, C.; Clifford, S.; Ochterski, J.; Petersson G. A.; Ayala P. Y.; Cui, Q.; Morokuma, K.; Malick, D. K.; Rabuck, A. D.; Raghavachari K.;, Foresman J. B.; Cioslowski J.; Ortiz J. V.; Baboul, A. G.; Stefanov B. B.; Liu, G.; Liashenko, A.; Piskorz, P.; Komaromi, I.; Gomperts R.; Martin, R. L.; Fox D. J.; Keith T.; Al-Laham M. A.; Peng C. Y.; Nanayakkara A.; Gonzales C.; Challacombe M.; Gill P. M. W.; Johnson B.; Chen W.; Wong M. W.; Andres J. L.; Head-Gordon M.; Replogle E. S.; Pople J. A. Gaussian, Inc., Pittsburgh, PA, 1998.
(24) March, J. *Advanced Organic Chemistry;* John Wiley: New York, 1992.
(25) Vargas R.; Garza J.; Dixon D. A.; Hay B. P. *J. Phys. Chem. A* **2000**, *104*, 5115.
(26) Mó, O.; Yañez, M.; Elguero, J. *J. Chem. Phys.* **1992**, *97*, 6628.
(27) Boyd, R. J.; Choi, S. C. *Chem. Phys. Lett.* **1985**, *120*, 80.
(28) Suzuki, S.; Green, P. G.; Bumgarner, R. E.; Dasgupta, S.; Goddard, W. A., III; Blake, G. A. *Science* **1992**, *257*, 942.
(29) Atwood, J. L.; Hamada, F.; Robinson, K. D.; Orr, G. W.; Vincent, R. L. *Nature* **1991**, *349*, 683.
(30) Steiner, T.; Starikov, E. B.; Amado, A. M.; Teixeira-Dias, J. J. C. *J. Chem. Soc., Perkin Trans. 2* **1995**, 1321.
(31) Steiner, T.; Lutz, B.; van der Maas, J.; Veldman, N.; Schreurs, A. M. M.; Kroon, J.; Kanters, J. A. *Chem. Commun.* **1997**, 191.
(32) Mallinson P. R.; Woźniak, K.; Wilson, C. C.; McCormack K. L.; Yufit, D. S. *J. Am. Chem. Soc.* **1999**, *121*, 4640.
(33) Nakagawa, N.; Fujiwara, S. *Bull. Chem. Soc. Jpn.* **1960**, *33*, 1634.
(34) Zushi, S.; Kodama, Y.; Nishihata, K.; Umemura, K.; Nishio, M.; Uzawa, J.; Hirota, M. *Bull. Chem. Soc. Jpn.* **1980**, *53*, 3631.
(35) Uzawa, J.; Zushi, S.; Kodama, Y.; Fukuda, Y.; Nishihata, K.; Umemura, K.; Nishio, M.; Hirota, M. *Bull. Chem. Soc. Jpn.* **1980**, *53*, 3623.
(36) Pople, J. A.; Frisch, M. J.; Del Bene, J. E. *Chem. Phys. Lett.* **1982**, *91*, 185.
(37) Frisch, M. J.; Pople, J. A.; Del Bene, J. E. *J. Chem. Phys.* **1983**, *78*, 4063.
(38) Sapse, A. M.; Jain, D. C. *J. Phys. Chem.* **1984**, *88*, 4970.
(39) Tang, T. H.; Hu, W. J.; Yan, D. Y.; Cui, Y. P. *J. Mol. Struct. (THEOCHEM)* **1990**, *207*, 319.
(40) Cubero, E.; Orozco, M.; Hobza, P.; Luque, F. J. *J. Phys. Chem. A* **1999**, *103*, 6394.
(41) Novoa, J. J.; Mota, F. *Chem. Phys. Lett.* **2000**, *318*, 345.
(42) Rzepa, M. S.; Webb, M. L.; Slawin, M. Z.; Williams D. J. *J. Chem. Soc., Chem. Commun.* **1991**, 765.
(43) Hanton, L. R.; Hunter, C. A.; Purvis, D. H. *J. Chem. Soc., Chem. Commun.* **1992**, 1134.
(44) Bondi, A. *J. Phys. Chem.* **1964**, *68*, 441.
(45) Hobza, P.; Špirko, V.; Selzle, H. L.; Schlag, E. W. *J. Phys. Chem. A* **1998**, *102*, 2501.
(46) Seiler P.; Dunitz J. *Helv. Chim. Acta* **1985**, *68*, 2093.
(47) Goddard. R.; Heinemann, O.; Krüger C. *Acta Crystallogr.* **1997**, *C53*, 590.
(48) Gu Y.; Kar, T.; Scheiner S. *J. Mol. Struct.* **2000**, *552*, 17.
(49) van der Veken, B. J.; Herrebout, W. A.; Szostak, R.; Shchepkin, D. N.; Havlas, Z.; Hobza, P. *J. Am. Chem. Soc.* **2001**, *123*, 12290.
(50) Grabowski, S. J. *J. Mol. Struct.* **2001**, *562*, 137.